ICAS-98-R,5,3

A98-31634

ANALYSIS OF THE INTERACTION EFFECT FOR BONDED REPAIRS

S.Sanderson, L.F.R.Rose and R.J.Callinan

Airframes and Engines Division, Defence Science & Technology Organisation - Aeronautical & Maritime Research Laboratory, 506 Lorimer Street, Fishermens Bend, Victoria 3207, Australia.

Abstract

With the increasing use of bonded repairs to restore the structural integrity of ageing aircraft the question arises as to the interaction effects when repairs are located close together. Using the Finite Element (F.E.) method a study has been carried out for the interaction between two idealised circular patches to repair cracks in thin skins. While circular patches are considered the same trends are expected for non-circular patches. The interaction involves the increase of the sheet stress just outside the patch. It has been found that the tandem orientation, with respect to the applied load, is the worst configuration. In this case, for most practical repairs, the interaction may result in increases of the sheet stress by 40% for very close separation distances. It has also been found that biaxial loading can also significantly influence the interaction effect.

Introduction

The repair of cracked aircraft structures using bonded repairs has resulted in considerable aircraft lifetime extension and hence cost savings. The long fatigue life of a bonded repair is attributed to the lack of rivets and hence stress concentrations in the repair. However the widespread use of these repairs for ageing aircraft may result in repairs located close together. The purpose of this study is to quantify the interaction effect. The existence of this effect has been shown in reference[1] for limited geometries. In the work carried out here, however, a parametric study is carried out. In this study the increase in the stress in the sheet just outside the patch is the quantity being considered. The orientation of the repairs is considered with respect to the applied load. Furthermore biaxial loadings will be considered. The finite width effect is also considered for two different configurations.

F.E. Methodology

The representation of the repair in this analysis is simplified and does not include the adhesive, in accordance with stage 1 of the two-stage design analysis proposed by Rose[2] for repair design. For convenience the reinforcement has been modelled to be a circular patch with constant thickness. Only in-plane loads are considered, and out-of-plane secondary bending has been restrained. Thus the analysis is most appropriate for two-sided repairs, or for cases where out-of-plane deflection is restrained by stiff sub-structure[3]; one-sided repairs introduce geometrical non-linearity and new length-scales which are not considered here[4]. Also it was assumed that the hole or crack being reinforced does not affect the load being drawn into the patch. As a result a simple model has been developed in which the variables are firstly the ratio of the combined Young's modulus of the patch and sheet beneath, E_0, to the sheet modulus, E_S, as indicated in Fig. 1, and secondly by the separation distance, $2S$, between the two repairs (Fig. 2). From equilibrium considerations the E_O / E_S ratio for any repair, as shown in Fig. 1, is given by:

$$\frac{E_O}{E_S} = \frac{E_S t_S + E_P t_P}{E_S t_S} \qquad (1)$$

where

E_P	Young's modulus for the patch
t_S	thickness of the sheet
t_P	thickness of the patch

For most repairs $E_P t_P = E_S t_S$, hence $E_O / E_S = 2$. For an over-stiff repair $E_P t_P > E_S t_S$

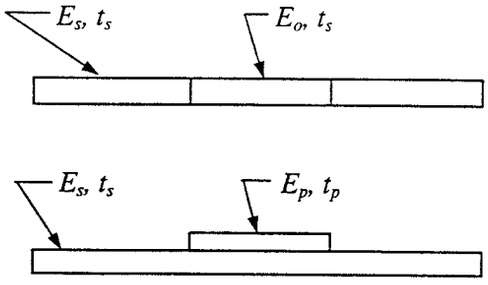

FIGURE 1. Geometry for equivalent stiffness representation.

Load cases considered are for remote σ_X and σ_Y stresses and a combination of both σ_X and σ_Y. The axis system used is shown in Fig. 2.

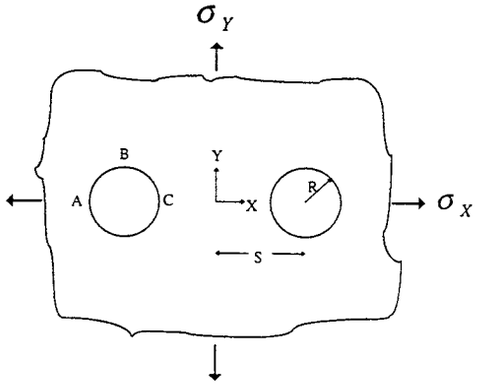

FIGURE 2 Two repairs in an infinite sheet: axis system and locations of interest.

The separation between the repairs is expressed as a ratio of S/R. Shown in Fig. 3. is a close up view of the F.E. mesh for a separation ratio of 1.1. A range of separation ratios of 1.1 to 5 will be considered.

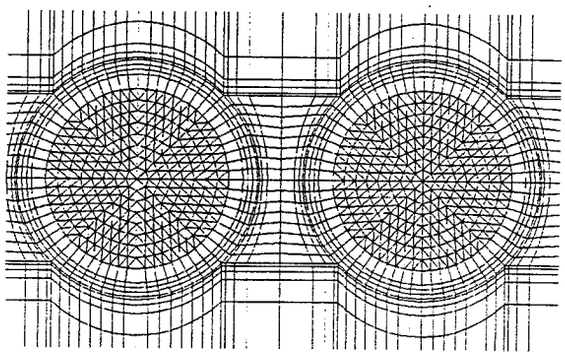

FIGURE 3 Close up view of mesh for S/R=1.1

Results

Firstly a convergence study was carried out to determine the fineness of the mesh required to give results for an accuracy of three significant figures at the points *A, B* and *C* shown in Fig. 2. These points have been identified as being the critical locations by graphical means. In all cases the maximum and minimum principal stresses, σ_1 and σ_2 were considered. Convergence to desired accuracy was achieved in all cases.

Tandem configuration

This configuration is shown in Fig. 4 and corresponds to an applied stress of $\sigma_X = 1$ and $\sigma_Y = 0$. The stress contours indicate that the maximum principal stress, σ_1, occurs at location C (see Fig. 2). Also it happens that the maximum principal stress occurs in the X direction. The results for this configuration with respect to the applied load are shown in Fig. 5 and indicate a strong interaction for close separation and high E_O / E_S values, and maximum stress ratio of 1.60 was achieved. Normally a repair would correspond to $E_O / E_S = 2$ and hence would correspond to a maximum S/R ratio of 1.4. At large separation distances σ_1 approaches an asymptotic value which corresponds to that of a single repair.

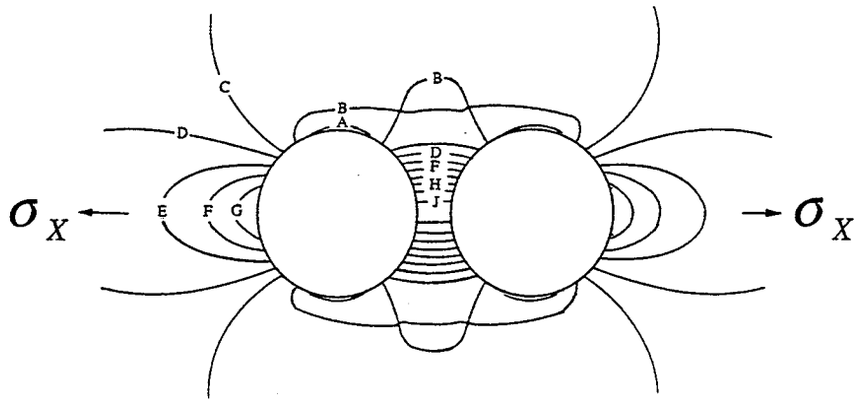

FIGURE 4. Tandem configuration: stress interaction between two circular repairs, where $\sigma=\sigma_x=1$ and S/R=1.2. (A=.878, B=.928, C=.977, D=1.027, E=1.076, F=1.126, G=1.175, H=1.225, I=1.274, J=1.324)

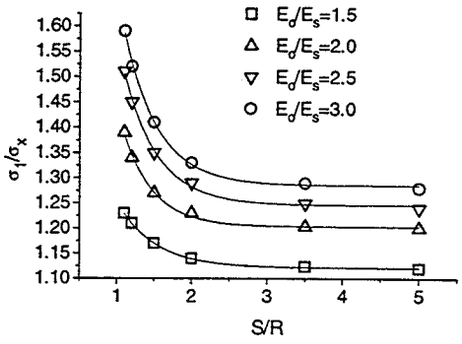

FIGURE 5 Tandem configuration: variation of stress ratio σ_1/σ_x with S/R ratio.

Side by side configuration

This configuration is shown in Fig. 6 and corresponds to the applied loading $\sigma_X = 0$ and $\sigma_Y = 1$. In this case the stress contours for the maximum principal stress show that the maximum value occurs at location B (see Fig. 2). Also it happens that the maximum principal stress occurs in the Y direction. The results for a study of the interaction are shown in Fig. 7. These results are different to the previous case in that the maximum stress ratios occur at large separations, due to shielding, and show an asymptotic behaviour. As before, the maximum stress concentration in the sheet occurs for high E_O / E_S values. The maximum stress ratio achieved was 1.28. Again, for most repairs ($E_O / E_S = 2.$) and the maximum stress ratio is 1.19.

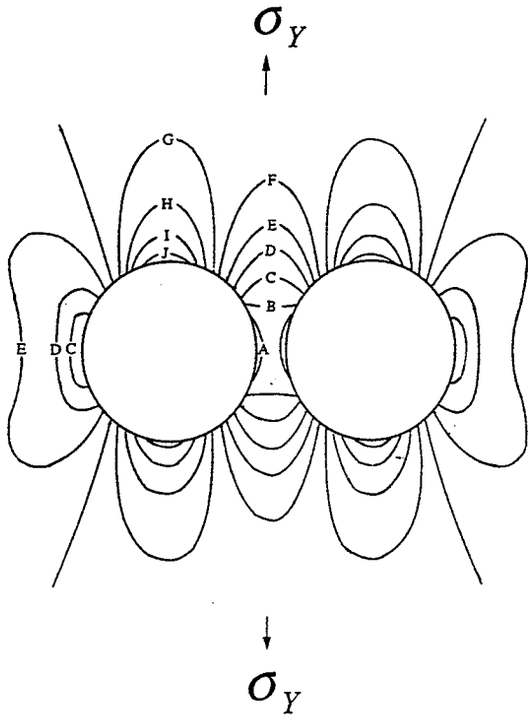

FIGURE 6. Side by side configuration: stress interaction between two circular repairs, where σ_x=1. and σ_y=0. and S/R=1.2 (A=.810, B=.848, C=.886, D=.925, E=.963, F=1.001, G=1.039, H=1.078, I=1.116, J=1.154)

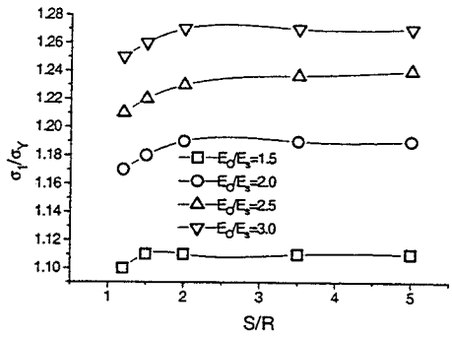

FIGURE 7. Side by side configuration: variation of stress ratio σ_1/σ_y with S/R ratio.

Periodic array

This is the representation of an infinite number of repairs in the X direction, as shown in Fig. 8, and is equivalent to the tandem configuration. The height of the sheet is very large in comparison to the radius, and hence can be assumed to be infinite. The loading is carried out by applying uniform displacements in the X direction along the face of the sheet. This results in a variation of σ_X stress in the Y direction and from this an average stress has been calculated. Results for a range of E_O / E_S are presented in Fig. 9 and correspond to point *A* shown in Fig 8. Although the separation distance is considered in terms of W/*R* ratio's, it is apparent that at close separations maximum stress ratio's of 1.9 are achieved at point *A*, with a value of $E_O / E_S = 3.0$.

Combination of loads

A bi-axial stress field has been considered in which the applied stresses are $\sigma_X = 1$ and $\sigma_Y = -1$, corresponding to the geometry in Fig. 1. These results are shown in Fig. 10. In this case the maximum interaction occurs at location C (see Fig. 2) corresponding to the lower *S/R* ratios. Again the repairs with large *Eo/Es* ratios result in the largest σ_1 / σ_X ratios. The maximum principal stress also happens to occur in the *X* direction. This combination of loads results in a stress interaction equal to that of the periodic array.

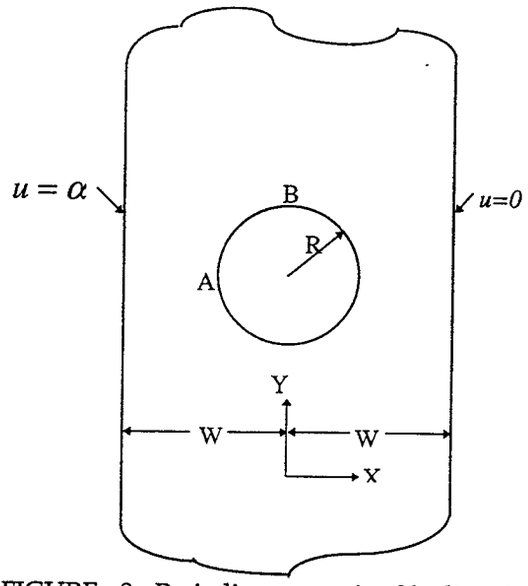

FIGURE 8 Periodic array in X direction (tandem configuration), infinite in Y direction.

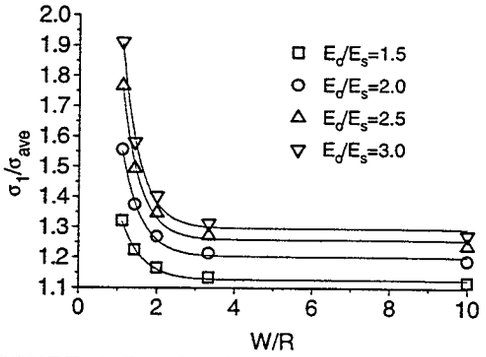

FIGURE 9 Results for periodic array, stress ratio σ_1/σ_{ave} for W/R ratios.

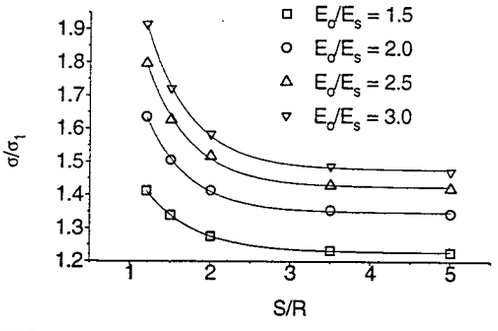

FIGURE 10. Bi-axial loading: S/R=1.1, σ_x=1, σ_y=-1, stress ratio at point C .

For the case where $\sigma_X = \sigma_Y = 1$, for the geometry shown in Fig. 1, results are shown in Fig. 11. In comparison to Fig. 5 for the uni-axial case, the combination of stresses alleviates the interaction effect. Clearly, the direction of the load components is important.

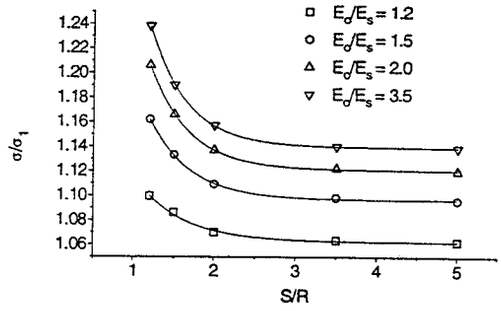

FIGURE 11. Bi-axial loading, S/R=1.1, σ_x=1, σ_y=1, stress ratio at point C.

Finite width effect

Consider the tandem configuration shown in Fig. 12. In this case the S/R ratio has been set to 1.1 since it is already known that the highest interaction occurs with this geometry. The results shown in Fig. 13 show a percentage change of sheet stress (location C) with a variation of width, W, (expressed as a ratio W/R). The greatest reduction in sheet stress occurs for W/R ratios approaching 1, and for higher E_O / E_S ratios.

For the case of the side by side configuration shown in Fig. 14 the S/R ratio adopted was 3 since the highest stress occurs at large separations. The results for the percentage change of sheet stress (location B) versus W/R are shown in Fig. 15. Again the largest reductions of sheet stress occur for W/R ratios approaching 1, and for higher E_O / E_S ratios. In comparison with the tandem configuration the finite width effect is not as strong. The results may be surprising that a smaller width should decrease the sheet stress, but an explanation is that with a narrow width the load attraction ability is limited.

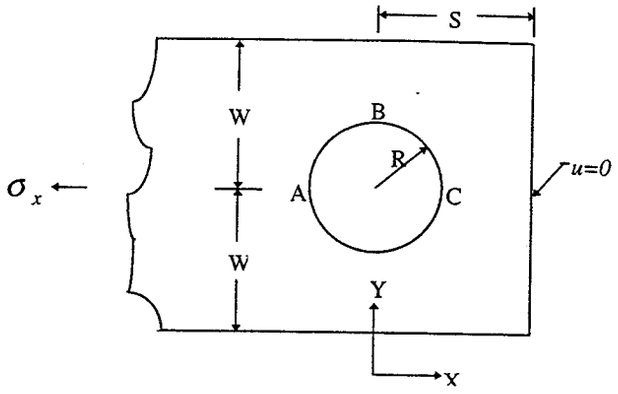

FIGURE 12. Finite width effect: tandem configuration.

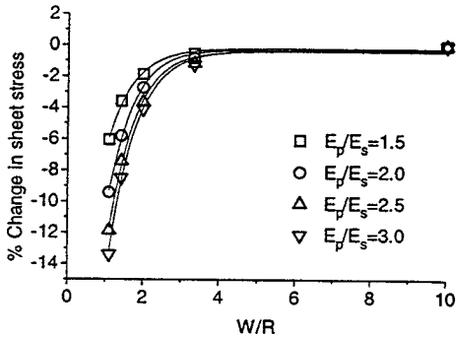

FIGURE 13. Finite width effect: % Change in sheet stress for tandem configuration.

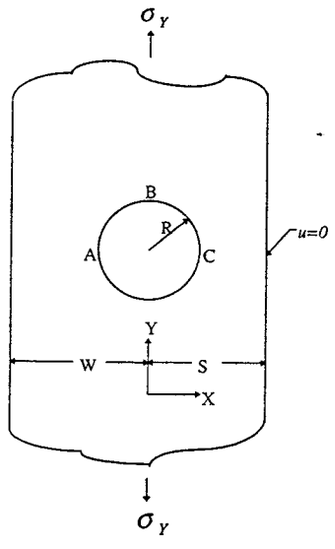

FIGURE 14. Finite width effect: side by side configuration.

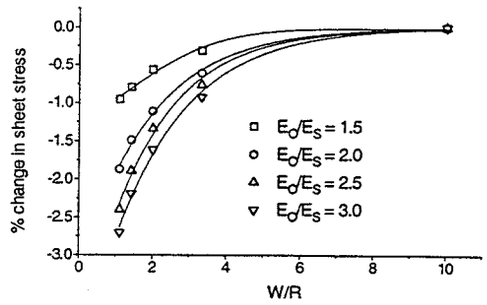

FIGURE 15. Finite width: % Change in sheet stress for side by side configuration.

Conclusion

Results indicate that maximum stress increases, depend on both the orientation of the repair with respect to the applied load, and separation distance between repairs. The side by side configuration with respect to the applied load gave stress increases of between 12-27%, where the maximum values occurred at the larger separation distances. In the case of the tandem configuration with respect to the applied load, stress increases of between 23-60% were obtained and the maximum correspond to small separation distances. In both orientations over stiff repairs gave the maximum stress increases. Thus, shielding and load-shedding behaviour for neighbouring repairs is in complete contrast to that for neighbouring holes or cutouts, which could be regarded as limiting cases for which $E_O/E_S \rightarrow 0$, whereas for repairs $E_O/E_S > 1$.

Bi-axial loading combinations can either increase or decrease the stress field interactions. If the applied component stresses are of the same sign interaction stresses are decreased; while applied stresses of opposite signs result in increased interaction stresses.

Results from the study of the periodic array in one direction have shown that this configuration gives the highest stress increases for uni-axial loading, and also is a tandem orientation with respect to the load. An investigation of the finite width effect has shown that repairs in sheets with small widths result in smaller stresses than in large width sheets. In this case the repair is no longer able to attract additional load from the surrounding structure.

References

1. W.T.Chow and S.N.Atluri Composite patch repairs of metal structures - Adhesive non-linearity. AIAA Journal, vol.35, no. 9, Sept 1997.

2. L.R.F.Rose Theoretical Analysis of Crack Patching, in Bonded Repair of Aircraft Structures, A.A. Baker and R. Jones (eds.), Martinus Nijhoff (1988).

3. L.R.F.Rose, R.J.Callinan, A.A.Baker, S.Sanderson and E.S.Wilson. Design Validation for a Bonded Composite Repair to the F-111 Lower Skin. PICAST-AAC6 Conference, Melbourne, March 20-23, 1995.

4. C.H.Wang, L.R.F.Rose and R.J.Callinan. Analysis of out-of-plane bending in one-sided bonded repair. Int. J. Solids Structures Vol. 35, No. 14, pp. 1653-1675, 1998.